

Aryldiazenido Complexes: Syntheses of Diiridium Complexes with Mono- and Dibridding Aryldiazenido Ligands and X-ray Structures of

$[(\eta^5\text{-C}_5\text{Me}_5)\text{IrI}]_2(\mu\text{-}\eta^2\text{-}p\text{-N}_2\text{C}_6\text{H}_4\text{OMe})(\mu\text{-}\eta^1\text{-}p\text{-N}_2\text{C}_6\text{H}_4\text{OMe})$ and $[\{(\eta^5\text{-C}_5\text{Me}_5)\text{Ir}(\text{CO})\}_2(\mu\text{-}\eta^2\text{-}p\text{-N}_2\text{C}_6\text{H}_4\text{OMe})][\text{BF}_4]^\dagger$

Xiaoqian Yan, Raymond J. Batchelor, Frederick W. B. Einstein, and Derek Sutton*

Department of Chemistry, Simon Fraser University, Burnaby, British Columbia, Canada V5A 1S6

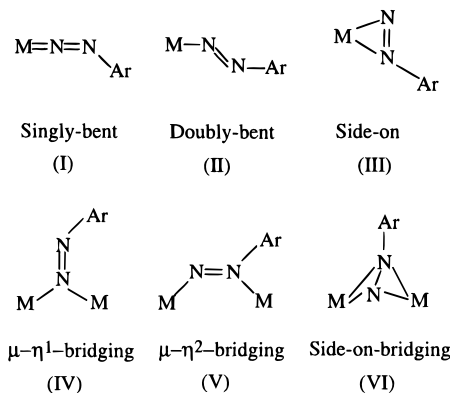
Received May 16, 1996[⊗]

The complex $[(\eta^5\text{-C}_5\text{Me}_5)\text{Ir}(\text{C}_2\text{H}_4)(p\text{-N}_2\text{C}_6\text{H}_4\text{OMe})][\text{BF}_4]$ (**1**) reacts with $\text{X}^- = \text{I}^-$ and Br^- to give neutral $[(\eta^5\text{-C}_5\text{Me}_5)\text{IrX}]_2(\mu\text{-}\eta^2\text{-}p\text{-N}_2\text{C}_6\text{H}_4\text{OMe})(\mu\text{-}\eta^1\text{-}p\text{-N}_2\text{C}_6\text{H}_4\text{OMe})$ where $\text{X} = \text{I}$ (**2**) and Br (**3**), respectively. The spectroscopic data for **2** and **3**, as well as their $^{15}\text{N}_\alpha$ derivatives **2a** and **3a**, establish that **2** and **3** are isostructural in solution and each contains diiridium centers that are bridged by two coordinatively different aryldiazenido ligands, i.e., $\mu\text{-}\eta^2\text{-}$ and $\mu\text{-}\eta^1\text{-}p\text{-N}_2\text{C}_6\text{H}_4\text{OMe}$ groups. This structural feature has also been unequivocally confirmed in the solid state by a single-crystal X-ray crystallographic analysis of **2**. The NMR studies of the protonation reactions of **2a** and **3a** indicate that protonation occurs solely at the N_α atom of the $\mu\text{-}\eta^2\text{-}p\text{-N}_2\text{C}_6\text{H}_4\text{OMe}$ ligand in both cases. When **1** reacts with the metal base complex $(\eta^5\text{-C}_5\text{Me}_5)\text{Ir}(\text{CO})_2$ in ethanol at reflux, the monobridging aryldiazenido complex $[\{(\eta^5\text{-C}_5\text{Me}_5)\text{Ir}(\text{CO})\}_2(\mu\text{-}\eta^2\text{-}p\text{-N}_2\text{C}_6\text{H}_4\text{OMe})][\text{BF}_4]$ (**6**) results. The molecular structure of **6** in the solid state, established by a single-crystal X-ray crystallographic analysis, is consistent with its spectroscopic properties in solution. On the basis of an EHMO calculation and a fragment orbital interaction analysis, a rationale is suggested to explain how the electronic nature of the substituent ligand influences the outcome of substitution reactions of **1**. Complex **2** crystallized in the space group $P\bar{1}$ with $a = 8.937(2)$ Å, $b = 10.036(2)$ Å, $c = 10.893(2)$ Å, $\alpha = 79.98(1)^\circ$, $\beta = 79.52(1)^\circ$, $\gamma = 70.36(1)^\circ$, and $Z = 1$. The structure of **2** was refined to $R_F = 0.021$ and $R_{wF} = 0.029$ on the basis of 3077 observed independent reflections with $I_o \geq 2.5\sigma(I_o)$ and 189 variables in the range $2\theta = 4\text{--}52^\circ$. Complex **6** crystallized in the space group $Pc2_1b$ with $a = 8.821(1)$ Å, $b = 20.237(2)$ Å, $c = 34.808(5)$ Å, and $Z = 8$. The structure of **6** was refined to $R_F = 0.044$ and $R_{wF} = 0.049$ on the basis of 1661 observed independent reflections with $I_o \geq 2.5\sigma(I_o)$ and 259 variables in the range $2\theta = 4\text{--}50^\circ$.

Introduction

The wide range of coordination geometries adopted by aryldiazenido ligands in complexes (Chart 1) has stimulated great interest in their structural study.¹ Of key importance is an understanding of the geometric and electronic requirements of the differently coordinated aryldiazenido ligands in complexes. Some effort has been made to obtain a general theoretical description of the electronic structure of the bonding in transition metal organodiazenido complexes.^{2–4a} However, little is known about how the molecular geometry, the properties of ancillary ligands, or, importantly, the geometrical disposition of the ancillary ligand in a given molecular geometry influence the metal–aryldiazenido bonding. We have been concerned with these questions, both in the experimental arena and in the theoretical domain.

Chart 1. Modes of Coordination of Aryldiazenido Ligands



In an earlier paper of this series we reported that the singly-bent aryldiazenido ligand, bound in an end-on coordination fashion (**I**), has unique anisotropic π electronic properties.^{4a} It has strong π -accepting ability only in the bending plane, whereas in the perpendicular direction it is a moderate π -donor. This “single-faced” π -accepting property of the aryldiazenido ligand has been used to satisfactorily rationalize the structure, fluxionality, and properties of the iridium aryldiazenido complexes $[\text{Cp}^*\text{Ir}(\text{L})(p\text{-N}_2\text{Ar})]^+$ ($\text{L} = \text{C}_2\text{H}_4$ (**1**), $\text{P}(p\text{-Tol})_3$); $\text{Cp}^* = \eta^5\text{-C}_5\text{Me}_5$; $\text{Ar} = \text{C}_6\text{H}_4\text{OMe}$).^{4,5}

Considering the importance of the π interaction in stabilizing the singly-bent aryldiazenido ligand in $[\text{Cp}^*\text{Ir}(\text{L})(p\text{-N}_2\text{Ar})]^+$, it

[†] Presented in part at 75th National Meeting of the Canadian Institute of Chemistry, Edmonton, Canada, 1992.

[⊗] Abstract published in *Advance ACS Abstracts*, November 15, 1996.

- (1) See: (a) Zollinger, H. *Diazo Chemistry II*; VCH: New York, 1995; p 421. (b) Sutton, D. *Chem. Rev.* **1993**, 93, 995. (c) Johnson, B. F. G.; Haymore, B. L.; Dilworth, J. R. In *Comprehensive Coordination Chemistry*; Wilkinson, G., Gillard, R. D., McCleverty, J. A., Eds.; Pergamon Press: Oxford, England, 1987; Vol. 2, p 130. (d) Niemeyer, H. M. In *The Chemistry of Diazonium and Diazo Groups*; Patai, S., Ed.; Wiley: New York, 1978; Vol. 1, Chapter 7. (e) Bruce, M. I.; Goodall, B. L. In *The Chemistry of Hydrazo, Azo, and Azoxy Groups*; Patai, S., Ed.; Wiley: Chichester, England, 1975; Part 1, Chapter 9. (f) Sutton, D. *Chem. Soc. Rev.* **1975**, 4, 443.
- (2) Dubois, D. L.; Hoffmann, R. *Nouv. J. Chim.* **1977**, 1, 479.
- (3) Moller, E.; Jorgensen, K. A. *Acta Chem. Scand.* **1991**, 45, 68.
- (4) (a) Yan, X.; Einstein, F. W. B.; Sutton, D. *Can. J. Chem.* **1995**, 73, 939. (b) Einstein, F. W. B.; Yan, X.; Sutton, D. *J. Chem. Soc., Chem. Commun.* **1990**, 1446.

- (5) Kim, G. C.; Batchelor, R. J.; Yan, X.; Einstein, F. W. B.; Sutton, D. *Inorg. Chem.* **1995**, 34, 6163.

was further anticipated that an increase of the energy of the filled metal d_{π} orbital of interest could result in electron transfer from the metal to the singly-bent aryldiazenido ligand, and consequently, a change in geometry of the aryldiazenido ligand from singly-bent to doubly-bent should be observed. In practice, this might be achieved either (i) by changing the molecular geometry from a two-legged piano stool structure to a three-legged one by introducing another suitable ligand or (ii) by changing the relative π -basicity of the ancillary ligand L. In illustration of the validity of proposal i, we very recently showed that a series of neutral and cationic doubly-bent aryldiazenido complexes can be obtained by coordinating a further, carefully selected, ligand to the singly-bent aryldiazenido compounds $[\text{Cp}^*\text{Ir}(\text{L})(p\text{-N}_2\text{Ar})]^+$.⁵

In this contribution, in pursuit of proposal ii, we report the results obtained by changing the ancillary ligand L to a π -base ligand, such as Br^- or I^- . In conjunction with previous papers of this series,⁴⁻⁶ we are able to demonstrate clearly the electronic effect that an ancillary ligand has on the geometric preference of the aryldiazenido ligand in these types of half-sandwich complexes. Despite numerous aryldiazenido complexes in the literature,¹ there are but a few with bridging aryldiazenido ligands.⁷ To our knowledge, the only other structurally determined complex containing a η^2 -bridging aryldiazenido ligand observed here⁸ is $(\mu\text{-H})\text{Os}_3(\text{CO})_{10}(\mu\text{-}\eta^2\text{-}p\text{-N}_2\text{Ph})$.^{7a} The facile geometric rearrangement of the aryldiazenido ligand from singly-bent to bridging, presented and rationalized in this work, provides a new synthetic route to rarely-encountered bridging aryldiazenido complexes.

Experimental Section

All solvents were dried and freshly distilled under nitrogen prior to use from sodium/benzophenone (diethyl ether), calcium hydride (dichloromethane), sodium (hexanes), or anhydrous calcium sulfate (ethanol). All preparations, reactions, and manipulations were carried out in standard Schlenk ware, connected to a switchable double manifold providing vacuum and nitrogen, unless otherwise noted.

Infrared spectra for solutions were measured in CaF_2 cells, and solid samples were measured as either KBr pellets or as a thin film on a KBr disk by using a Bomem Michelson 120 FTIR instrument. Some of the routine ^1H NMR spectra were recorded at 100 MHz by using a Bruker SY-100 spectrometer. The remaining ^1H NMR and ^{15}N NMR spectra were obtained in the NMR service of Simon Fraser University by Mrs. M. Tracey on a Bruker AMX-400 instrument at operating frequencies of 400.1 and 40.5 MHz for ^1H and ^{15}N , respectively. Chemical shifts (δ) are reported in ppm, downfield positive, relative to tetramethylsilane (TMS) for ^1H and relative to external MeNO_2 for ^{15}N spectra. Coupling constants are reported in hertz. Fast atom bombardment (FAB) or electron impact (EI) mass spectra were obtained by Mr. G. Owen on a Hewlett-Packard Model 5985 GC-MS spectrometer equipped with a fast atom bombardment probe (xenon source, Phrasor Scientific, Inc., accessory) and utilized samples dispersed or dissolved in thioglycerol. The pattern of the envelopes of the fragment ions were matched with that simulated by computer for the species in question, and in all cases the m/z value quoted is that for the most

intense peak. Microanalyses for C, H, N were performed by Mr. M.-K. Yang of the Microanalytical Laboratory of Simon Fraser University. The melting points were recorded by using a Fisher-Johns melting point apparatus and are uncorrected.

p-Methoxybenzenediazonium tetrafluoroborate was prepared by the standard procedure using *p*-methoxyaniline (Aldrich) and sodium nitrite and purified periodically by recrystallization from acetone and diethyl ether. The diazonium salt substituted with ^{15}N at the terminal nitrogen (N_α) was prepared by using $\text{Na}^{15}\text{NO}_2$ (95% ^{15}N , MSD Isotopes) and was employed for the syntheses of ^{15}N -labeled compounds. (Pentamethylcyclopentadienyl)iridium dicarbonyl was synthesized either by the Maitlis method⁹ or by a method developed in this laboratory.¹⁰ The syntheses of $[\text{Cp}^*\text{Ir}(\text{C}_2\text{H}_4)(p\text{-N}_2\text{C}_6\text{H}_4\text{OMe})][\text{BF}_4]$ (**1**) and its isotopomer $[\text{Cp}^*\text{Ir}(\text{C}_2\text{H}_4)(p\text{-}^{15}\text{N}_\alpha\text{NC}_6\text{H}_4\text{OMe})][\text{BF}_4]$ (**1a**) were reported previously.⁴

Preparation of $[\text{Cp}^*\text{Ir}]_2(\mu\text{-}\eta^2\text{-}p\text{-N}_2\text{C}_6\text{H}_4\text{OMe})(\mu\text{-}\eta^1\text{-}p\text{-N}_2\text{C}_6\text{H}_4\text{OMe})$ (2**).** To a solution of $[\text{Cp}^*\text{Ir}(\text{C}_2\text{H}_4)(p\text{-N}_2\text{C}_6\text{H}_4\text{OMe})][\text{BF}_4]$ (**1**) (50 mg, 0.061 mmol) in 10 mL of ethanol was added an equimolar amount of ground predried KI. The reaction mixture was vigorously stirred for ca. 2 h at room temperature. The color of the solution changed from yellow to brown, and a large amount of fine dark brown precipitate was produced. After removal of the solvent *in vacuo* at room temperature, the solid residue was redissolved in ca. 10 mL of $\text{CH}_2\text{-Cl}_2$, giving a brownish green solution and some fine white precipitate (KBF_4). Following filtration, the filtrate was evaporated to dryness, affording analytically pure compound **2** quantitatively. Recrystallization of **2** from CH_2Cl_2 /hexanes at -10°C gave cuboid-shaped dark brown crystals in higher than 90% yield. MP: 224°C dec. ^1H NMR (CDCl_3): δ 1.29 (s, 15H, C_5Me_5), 1.37 (s, 15H, C_5Me_5), 3.84 (s, 6H, OMe), 6.85 (d, 2H, $J = 9$ Hz, aromatic), 6.96 (d, 2H, $J = 9$ Hz, aromatic), 7.74 (d, 4H, $J = 9$ Hz, aromatic). EIMS (m/z): 590 ($[\text{Cp}^*\text{Ir}(\text{N}_2\text{C}_6\text{H}_4\text{OMe})]^+$), 582 ($[\text{Cp}^*\text{Ir}_2]^+$), 562 ($[\text{Cp}^*\text{Ir}(\text{C}_6\text{H}_4\text{OMe})]^+$), 455 ($[\text{Cp}^*\text{Ir}]^+$). Anal. Calcd: C, 34.64; H, 3.76; N, 4.75. Found: C, 34.54; H, 3.77; N, 4.73.

Preparation of $[\text{Cp}^*\text{Ir}]_2(\mu\text{-}\eta^2\text{-}p\text{-}^{15}\text{NNC}_6\text{H}_4\text{OMe})(\mu\text{-}\eta^1\text{-}p\text{-}^{15}\text{NNC}_6\text{H}_4\text{OMe})$ (2a**).** The $^{15}\text{N}_\alpha$ -substituted complex **2a** was synthesized analogously to compound **2** by using $[\text{Cp}^*\text{Ir}(\text{C}_2\text{H}_4)(p\text{-}^{15}\text{N}_\alpha\text{NC}_6\text{H}_4\text{OMe})][\text{BF}_4]$ (**1a**). ^{15}N NMR (CDCl_3): δ 64.12 (s, N_α), 300.03 (s, N'_α).

Preparation of $[\text{Cp}^*\text{IrBr}]_2(\mu\text{-}\eta^2\text{-}p\text{-N}_2\text{C}_6\text{H}_4\text{OMe})(\mu\text{-}\eta^1\text{-}p\text{-N}_2\text{C}_6\text{H}_4\text{OMe})$ (3**).** A procedure similar to that used for **2**, but using predried KBr and a rather longer time (ca. 4 h), gave **3** quantitatively as dark brown microcrystals. ^1H NMR (CDCl_3): δ 1.22 (s, 15H, C_5Me_5), 1.28 (s, 15H, C_5Me_5), 3.86 (s, 6H, OMe), 6.85 (d, 2H, $J = 9$ Hz, aromatic), 6.95 (d, 2H, $J = 9$ Hz, aromatic), 7.79 (d, 4H, $J = 9$ Hz, aromatic). EIMS (m/z): 542 ($[\text{Cp}^*\text{IrBr}(\text{N}_2\text{C}_6\text{H}_4\text{OMe})]^+$), 488 ($[\text{Cp}^*\text{IrBr}_2]^+$), 463 ($[\text{Cp}^*\text{Ir}(\text{N}_2\text{C}_6\text{H}_4\text{OMe})]^+$), 407 ($[\text{Cp}^*\text{IrBr}]^+$). Anal. Calcd: C, 37.64; H, 4.09; N, 5.16. Found: C, 38.08; H, 4.11; N, 5.09.

Preparation of $[\text{Cp}^*\text{IrBr}]_2(\mu\text{-}\eta^2\text{-}p\text{-}^{15}\text{NNC}_6\text{H}_4\text{OMe})(\mu\text{-}\eta^1\text{-}p\text{-}^{15}\text{NNC}_6\text{H}_4\text{OMe})$ (3a**).** The $^{15}\text{N}_\alpha$ -substituted complex **3a** was synthesized analogously to compound **3** by using $[\text{Cp}^*\text{Ir}(\text{C}_2\text{H}_4)(p\text{-}^{15}\text{N}_\alpha\text{NC}_6\text{H}_4\text{OMe})][\text{BF}_4]$ (**1a**). ^{15}N NMR (CDCl_3): δ 69.84 (s, N_α), 303.44 (s, N'_α).

Observation of $\{[\text{Cp}^*\text{Ir}]_2(\mu\text{-}\eta^2\text{-}p\text{-}^{15}\text{N}_\alpha\text{HNC}_6\text{H}_4\text{OMe})(\mu\text{-}\eta^1\text{-}p\text{-}^{15}\text{NNC}_6\text{H}_4\text{OMe})\}[\text{BF}_4]$ (4**) by protonation of **2a**.** To a solution of **2a** (30 mg, 0.025 mmol) in 1 mL of CDCl_3 in a 2.5 mm diameter NMR tube was added ~ 0.1 mL (2 drops) of $\text{HBF}_4/\text{Et}_2\text{O}$ at room temperature. The solution became cloudy, but the precipitate redissolved on addition of two drops of acetone- d_6 . A ^{15}N NMR spectrum followed by a ^1H NMR spectrum was immediately recorded. ^1H NMR ($\text{CDCl}_3 + \text{acetone-}d_6$): δ 1.62 (s, 15H, C_5Me_5), 2.00 (s, 15H, C_5Me_5), 3.84 (s, 6H, OMe), 7.06 (m, 6H, aromatic), 8.20 (d, 1H, $J = 9$ Hz, aromatic), 8.33 (d, 1H, $J = 9$ Hz, aromatic), 15.20 (d, 1H, $J^{15\text{N-H}} = 79$ Hz, $^{15}\text{N}_\alpha\text{H}$). ^{15}N NMR ($\text{CDCl}_3 + \text{acetone-}d_6$): δ 65.1 (s, $^{15}\text{N}_\alpha$), -110.7 (s, b, $^{15}\text{N}_\alpha\text{H}$).

Observation of $\{[\text{Cp}^*\text{IrBr}]_2(\mu\text{-}\eta^2\text{-}p\text{-}^{15}\text{N}_\alpha\text{HNC}_6\text{H}_4\text{OMe})(\mu\text{-}\eta^1\text{-}p\text{-N}_2\text{C}_6\text{H}_4\text{OMe})\}[\text{BF}_4]$ (5**) by protonation of **3a**.** To a solution of **3a** (30 mg, 0.028 mmol) in ca. 2 mL CDCl_3 was added 0.1 mL (2 drops) of $\text{HBF}_4/\text{Et}_2\text{O}$ at room temperature. After mixing, the solution became cloudy and was filtered, and the filtrate was collected in a 2.5 mm diameter NMR tube. ^1H NMR (CDCl_3): δ 1.51 (s, 15H, C_5Me_5), 1.90

(6) (a) Cusanelli, A.; Batchelor, R. J.; Einstein, F. W. B.; Sutton, D. *Organometallics* **1994**, *13*, 5096. (b) Garcia-Minsal, A.; Sutton, D. *Organometallics* **1996**, *15*, 332.

(7) (a) Samkoff, D. E.; Shapley, J. R.; Churchill, M. R.; Wasserman, H. J. *Inorg. Chem.* **1984**, *23*, 397. (b) Einstein, F. W. B.; Sutton, D.; Vogel, P. L. *Inorg. Nucl. Chem. Lett.* **1976**, *12*, 671. (c) Dobinson, G. C.; Mason, R.; Robertson, G. B.; Ugo, R.; Conti, F.; Morelli, D.; Cenini, S.; Bonati, F. *J. Chem. Soc., Chem. Commun.* **1967**, 739. (d) Churchill, M. R.; Lin, K. G. *Inorg. Chem.* **1975**, *14*, 1133. (e) Churchill, M. R.; Wasserman, H. J. *Inorg. Chem.* **1981**, *20*, 1580. (f) Bruce, M. I.; Horn, E.; Snow, M. R.; Williams, M. L. *J. Organomet. Chem.* **1984**, *276*, C53. (g) Bruce, M. I.; Williams, M. L.; Skelton, B. W.; White, A. J. *Organomet. Chem.* **1986**, *309*, 157. (h) DeBlois, R. E.; Rheingold, A. L.; Samkoff, D. E. *Inorg. Chem.* **1988**, *27*, 3506.

(8) The structure of complex **6** was briefly reported previously.^{4b}

(9) Kang, J. W.; Moseley, K.; Maitlis, P. M. *J. Am. Chem. Soc.* **1969**, *91*, 5970.

(10) Yan, X. Ph.D. Thesis, Simon Fraser University, 1993.

Table 1. Crystallographic Data for the Structure Determination of Complexes **2** and **6**

	2	6
formula	Ir ₂ I ₂ O ₂ N ₄ C ₃₄ H ₄₄	Ir ₂ F ₄ O ₃ N ₂ C ₂₉ BH ₃₇
crystal system	triclinic	orthorhombic
space group	<i>P</i> $\bar{1}$	<i>Pc</i> 2 ₁ <i>b</i> ^a
<i>a</i> (Å)	8.937(2)	8.821(1)
<i>b</i> (Å)	10.036(2)	20.237(2)
<i>c</i> (Å)	10.893(2)	34.808(5)
α (deg)	79.98(1)	
β (deg)	79.52(1)	
γ (deg)	70.36(1)	
<i>Z</i>	1	8
<i>T</i> (K)	293	233
ρ (g/cm ³)	2.180	1.995
μ (MoK α) (cm ⁻¹)	91.1	85.9
crystal size (mm)	0.27 × 0.22 × 0.17	0.34 × 0.26 × 0.11
λ (Å)	0.71069	0.71069
transm	0.113–0.261	0.219–0.376
min–max 2θ (deg)	4–52	4–50
scan type	2θ	ω – 2θ
<i>R</i> _F ^b	0.021	0.044
<i>R</i> _{wF} ^c	0.029	0.049
GOF ^d	1.74	1.10

^a Nonstandard orientation with general equivalent points: *x*, *y*, *z*; $-x$, $y + 1/2$, $-z$; x , $y + 1/2$, $1/2 - z$; $-x$, *y*, $z + 1/2$. ^b $R_F = \sum(|F_o| - |F_c|) / \sum|F_o|$ for observed data. ^c $R_{wF} = [\sum w(|F_o| - |F_c|)^2 / \sum w|F_o|^2]^{1/2}$ for observed data. ^d $GOF = [\sum w(|F_o| - |F_c|)^2 / \text{degrees of freedom}]^{1/2}$.

(s, 15H, C₅Me₅), 3.84 (s, 6H, OMe), 6.89–7.41 (m, 6H, aromatic), 8.20 (d, 1H, *J* = 9 Hz, aromatic), 8.43 (d, 1H, *J* = 9 Hz, aromatic), 15.32 (d, 1H, *J*_{N–H} = 79 Hz, ¹⁵N_H).

X-ray Structure Determination of [Cp*IrI]₂(μ - η^2 -*p*-N₂C₆H₄OMe)(μ - η^1 -*p*-N₂C₆H₄OMe) (2**).** A red crystal of [Cp*IrI]₂(μ - η^2 -*p*-N₂C₆H₄OMe)(μ - η^1 -*p*-N₂C₆H₄OMe) (**2**), obtained by crystallization from CH₂-Cl₂/hexanes, was mounted on a glass fiber using epoxy resin adhesive. Intensity data (Mo K α radiation, graphite monochromator) were collected using an Enraf-Nonius CAD-4F diffractometer. The intensities were corrected for absorption by the Gaussian integration method (checked against measured ψ scans). Two intensity standards were measured every hour and decayed by 4% during the course of the measurements. Data reduction included corrections for intensity scale variation and for Lorentz and polarization effects. The final unit cell was determined from 25 reflections with $39^\circ < 2\theta < 50^\circ$.

The iridium atom position was derived from the Patterson map, and the rest of the non-hydrogen atom positions were located in subsequent Fourier maps. Disorder in the region of the bridging aryldiazenido ligand indicated two different bonding modes for this group. This is of course consistent with *Z* = 1 and a space group of *P* $\bar{1}$. The possibility of the space group being *P*1 was carefully examined, including measurement of 50 (predicted) largest Friedel nonequivalences. The treatment of the disorder is described in detail in the Supporting Information provided. Final full-matrix least-squares refinement included 189 parameters for 3077 data ($I_o \geq 2.5\sigma(I_o)$) and 52 restraints. An extinction coefficient¹¹ of 0.055(7) μm was also refined. The maximum residue of electron density in the final density map is 0.72(2) e/Å³ and is 0.99 Å from Ir. A weighting scheme, based on counting statistics, was applied such that $\langle w(|F_o| - |F_c|)^2 \rangle$ ($w = [\sum(|F_o|^2 + 0.0001(|F_o|)^2)]^{-1}$) was nearly constant as a function of both $|F_o|$ and $(\sin \theta)/\lambda$.¹¹ The pertinent crystallographic and experimental data for **2** are summarized in Table 1.

Complex scattering factors for neutral atoms¹² were used in the calculation of structure factors. The programs used for data reduction, structure solution, and initial refinement were from the NRCVAX Crystal Structure System.¹³ The program suite CRYSTALS¹⁴ was employed in the final refinement. All computations were carried out on a MicroVAX-II computer.

Preparation of [Cp*Ir(CO)]₂(μ - η^2 -*p*-N₂C₆H₄OMe)[BF₄] (6**).** A yellow ethanol solution (10 mL) of [Cp*Ir(C₂H₄)(*p*-N₂C₆H₄OMe)][BF₄] (**1**) (20 mg, 0.035 mmol) and Cp*Ir(CO)₂ (13 mg, 0.035 mmol) in a 50 mL pear-shaped flask equipped with a condenser was refluxed under a nitrogen atmosphere. IR monitoring of the reaction indicated that **1** was completely consumed in about 12 h. The dark red solution was cooled to room temperature, transferred to a Schlenk tube, and concentrated *in vacuo* to about 3 mL; then excess diethyl ether was added to precipitate the brownish product. Recrystallization of this product from acetone/diethyl ether gave ruby red crystals of compound **6** in 10% yield. IR $\nu(\text{CO})$: 1922, 1970 cm⁻¹ (KBr). ¹H NMR (CDCl₃): δ 2.13 (s, 15H, Cp*), 2.01 (s, 15H, Cp*), 3.89 (s, 3H, OMe), 7.05 (q, 4H, AA'BB' pattern, C₆H₄). FABMS (*m/z*): 845 (M⁺), 817 (M⁺ - CO or M⁺ - N₂), 789 (M⁺ - 2CO or M⁺ - CO - N₂), 761 (M⁺ - 2CO - N₂), 463 ([Cp*Ir(N₂C₆H₄OMe)]⁺). Anal. Calcd: C, 37.34; H, 4.00; N, 3.00. Found: C, 37.46; H, 4.06; N, 3.24.

Single-Crystal X-ray Crystallographic Analysis of [Cp*Ir(CO)]₂(μ - η^2 -*p*-N₂C₆H₄OMe)[BF₄] (6**).** Intensity data were collected at -40°C on an Enraf-Nonius CAD4-F diffractometer with graphite-monochromatized Mo K α radiation. The final unit cell was determined by least squares from the setting angles of 25 carefully centered reflections (with $26^\circ \leq 2\theta \leq 41^\circ$) chosen from a variety of well-spaced points in reciprocal space. An orthorhombic unit cell was first assumed and then confirmed by investigation of the symmetry-related reflections. The pertinent crystallographic and experimental parameters of **6** are given in Table 1.

A total of 3438 unique reflections were measured, of which 1661 reflections were classed as observed ($I_o \geq 2.5\sigma(I_o)$) and used in structure calculations and refinements. Two intensity standards were measured every 1.5 h of acquisition time and showed no significant change in intensity during the data collection process. A Gaussian intergration method based upon the crystal shape was used for absorption correction, and it was checked against the measured ψ -scan data based on four high-angle reflections with $\chi > 84^\circ$. Lorentz and polarization corrections were applied.

The Patterson method was used to solve the structure initially in the space group *Pc*mb. Refinement converged to *ca.* $R_F = 0.10$. Significantly, the thermal motion parameters and some interatomic distances were physically unreasonable in this model. The structure was then refined to $R_F = 0.08$ in the noncentric space group *Pc*2₁*b*, and a model involving disorder was required (the major molecular site had 85% occupancy). The details of the refinement are described in the Supporting Information provided. The refinement was considered complete when shift/esd ≤ 0.01 . In the final refinement, 305 atoms and 259 variables were included against 1661 observed independent reflections and gave final values of $R_F = 0.044$, $R_{wF} = 0.049$. The largest peak in the final electron density difference map was 1.2 e Å⁻³, 0.96 Å from Ir(1).

Unit weights were employed. Computations were carried out on a Micro VAX-II computer. The programs used for the absorption corrections, data reduction, structure solution, and graphical output were from the NRCVAX Crystal Structure System.¹³ Refinement was carried out using CRYSTALS.¹⁴ Complex scattering factors for neutral atoms¹² were used in the calculation of the structure factors.

Results and Discussion

Syntheses and Characterization of [Cp*IrX]₂(μ - η^2 -*p*-N₂C₆H₄OMe)(μ - η^1 -*p*-N₂C₆H₄OMe) (X** = **I** (**2**), **Br** (**3**)).** Previously, we have shown that the ethylene ligand in **1** is substitutionally labilized by the presence of the singly-bent aryldiazenido ligand in this type of two-legged piano stool molecule.^{4,5} This lability is also reflected here by the ready substitution by the halides I⁻ and Br⁻. Treatment of **1** with an equimolar amount of KI in ethanol leads to quantitative formation of the diiridium complex [Cp*IrI]₂(μ - η^2 -*p*-N₂C₆H₄OMe)

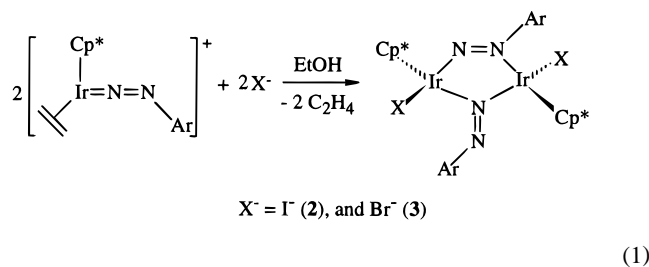
(11) Larson, A. C. In *Crystallographic Computing*; Ahmed, F. R., Ed.; Munksgaard: Copenhagen, 1970; p 291.

(12) *International Tables for X-ray Crystallography*; Kynoch Press: Birmingham, England, 1975; Vol. IV, p 99.

(13) Gabe, E. J.; LePage, Y.; Charland, J.-P.; Lee, F. L.; White, P. S. J. *Appl. Crystallogr.* **1989**, *22*, 384.

(14) Watkin, D. J.; Carruthers, J. R.; Betteridge, P. W. *CRYSTALS*; Chemical Crystallography Laboratory, University of Oxford: Oxford, England, 1984.

OMe)(μ - η^1 - p -N₂C₆H₄OMe) (**2**). The corresponding bromo complex **3** was synthesized in a similar way (eq 1) but required



a slightly longer reaction time. The use of KI or KBr instead of more soluble sources of halide in these reactions avoids a high initial solution concentration of halide, since this may cause substitution of the aryldiazenido ligand to form (Cp*IrX₂)₂.¹⁵

Attempts to prepare the chloro and alkoxy analogues by similar reactions of **1** with MCl and MOR (M = Li, Na, K; R = H, Me, Et), respectively, have been unsuccessful. For example, reaction of **1** with chlorides led mainly to (Cp*IrCl₂)₂,⁹ plus uncharacterized components, but no presence of an aryldiazenido ligand could be detected by IR and NMR.

Compounds **2** and **3** are very soluble in CH₂Cl₂, CHCl₃, and acetone and slightly soluble in EtOH and Et₂O. They are stable as solids and in solution, even in halogenated solvents, which contrasts sharply with the behavior of **1**. Satisfactory elemental analyses indicate both **2** (X = I) and **3** (X = Br) have an empirical formula Cp*IrX(N₂C₆H₄OMe). However, the solution infrared spectra of **2** and **3** show no bands assignable to ν (NN) in the ranges expected for a singly-bent or a doubly-bent aryldiazenido ligand.^{1c,16} No absorptions shift significantly in the IR spectra of **2a** or **3a** synthesized by using ¹⁵N_α-enriched **1**. In the EIMS it was not possible to observe the parent ions for **2** and **3** within the limited range our instrumentation. The highest m/z values observed were those for the monomeric ions [Cp*IrX(N₂C₆H₄OMe)]⁺ (X = I, Br), and the isotopic patterns agreed with the simulated ones, rather than those of the possible doubly-charged parents, i.e., [Cp*₂Ir₂X₂(N₂C₆H₄OMe)₂]²⁺, that would appear in the same m/z regions. The proton NMR spectrum of **2** in CDCl₃ shows two sharp singlets in the methyl group region (δ 1.29 and 1.37) and two separate, equal-intensity AA'BB' patterns in the aromatic region, indicative of two inequivalent Cp* groups and two inequivalent C₆H₄OMe groups, respectively. The proton NMR spectrum of **3** is similar. Significantly, the ¹⁵N NMR spectra of **2a** and **3a** unequivocally show the presence of two coordinatively distinct aryldiazenido ligands, one of which gives a resonance at δ 64.12 for **2a** (δ 69.84 for **3a**) and the other of which gives a resonance at δ 300.03 for **2a** (δ 303.44 for **3a**). The downfield signal at δ ~300 is in the region observed for N_α in doubly-bent terminal aryldiazenido ligands (**II**; Chart 1) but may also be compared with the N_α shift for the η^2 -bridging ligand (**V**; Chart 1) in (μ -H)Os₃(CO)₁₀(μ - η^2 - p -N₂C₆H₄Me) reported at δ 313.^{7a} The anomalous deshielding is attributed to the high-lying (in energy) lone pair at the N_α nucleus in either case.^{16,17} The signal occurring at relatively high field with δ ~60–70 is in the typical chemical shift range for a terminal singly-bent aryldiazenido ligand (**I**; Chart 1). This assignment is, however, not supported

by the absence of the characteristic strong ν (NN) IR absorption expected for this ligand. The η^1 -bridging aryldiazenido ligand (**IV**; Chart 1) in (μ -H)Os₃(CO)₁₀(μ - η^1 - p -N₂C₆H₄Me) exhibits a ¹⁵N_α chemical shift at δ 68, clearly in the same region as that of **2a** and **3a**.^{7a} Taken in conjunction with the X-ray solid state structure (vide infra), the two ¹⁵N_α resonances are assigned to the presence of an η^1 -bridging (δ ~60–70) and an η^2 -bridging (δ ~300) aryldiazenido ligand in the structures of **2** and **3** in solution, as illustrated in eq 1.

The ¹H and ¹⁵N NMR data could also be interpreted to indicate that **2** and **3** are 1:1 mixtures of two *different* symmetrical dimeric molecules, in one of which the bridging ligands are both η^1 and in the other both η^2 . This possibility is not supported by the X-ray structure or by the results of protonation of **2** and **3** and it is improbable that such isomers should have equal populations in solution. Note that the solution IR and NMR results indicate that **2** and **3** are not detectably dissociated into the monomers [Cp*IrX(N₂C₆H₄OMe)].

It should be noted at this point that formation of **2** or **3** in these reactions differs significantly from previously reported substitution reactions of **1** with π -acid ligands, such as triorganophosphines (see Scheme 2 below). Thus, when a bulky phosphine ligand (L) such as PPh₃ or P(*p*-tol)₃ was used, a monomeric product [Cp*Ir(L)(*p*-N₂C₆H₄OMe)]⁺ similar to **1** was always obtained.^{4,5} That is to say, the aryldiazenido ligand in these complexes remains singly-bent (**I**; Chart 1) as in **1**. However, when PMe₃ was used, no singly-bent aryldiazenido compound could be isolated. Instead, the bis(trimethylphosphine) complex [Cp*Ir(PMe₃)₂(*p*-N₂C₆H₄OMe)]⁺, containing a doubly-bent aryldiazenido ligand (**II**; Chart 1), was obtained.⁵ Similar doubly-bent aryldiazenido complexes were also formed by using the bidentate phosphine [Ph₂PCH₂]₂, as well as by addition of PMe₃, CO, CN⁻, and even H⁻ to the singly-bent aryldiazenido complex [Cp*Ir(PPh₃)(*p*-N₂C₆H₄OMe)]⁺.^{4,5} It seems probable that formation of the singly-bent aryldiazenido complex [Cp*Ir(PR₃)(*p*-N₂C₆H₄OMe)]⁺ by substitution of ethylene in **1** by a single phosphorus always occurred, and the addition of a second ligand (with concomitant structural isomerization of the *p*-N₂C₆H₄OMe ligand from singly- to doubly-bent) only occurs if compatible with the combined steric properties of the phosphine and incoming ligand. In the present case of substitution of C₂H₄ in **1** by the π -base ligands I⁻ and Br⁻, it is notable that the simple substitution products Cp*IrX(*p*-N₂Ar), which would be 18e complexes with singly-bent aryldiazenido ligands, are not observed. The outcome of ethylene substitution in **1** is thus extremely sensitive to the electronic as well as the steric properties of the incoming ligand and will be discussed in the context of the possible mechanism in a subsequent section.

X-ray Crystal Structure of [Cp*IrI]₂(μ - η^2 - p -N₂C₆H₄OMe)-(μ - η^1 - p -N₂C₆H₄OMe) (2**).** In the structure of **2** each unit cell contains one disordered dinuclear molecule lying on the inversion center of the centrosymmetric space group $P\bar{1}$. The configuration of each Ir is tetrahedral, and the Cp* groups are mutually trans, as are the terminal iodines. Interestingly, the disorder is only clearly evident in the region of the nitrogen atoms and is consistent with the superposition of two different bridging aryldiazenido ligands (**IV** and **V**; Chart 1) with equal occupancies. There is no observable disorder in the Cp*, the Ir, and the terminal iodine regions, as indicated by the well-behaved thermal motions for these groups in the final model and by the absence of any significant residual electron density in these regions in the final difference map.

The observed disordered structure of **2** could, in principle, result in two ways (Chart 2). Combination I postulates only

- (15) (a) Booth, B. L.; Haszeldine, R. N.; Hill, M. J. *Organomet. Chem.* **1969**, *16*, 491. (b) Gill, D. S.; Maitlis, P. M. *J. Organomet. Chem.* **1975**, *87*, 359.
- (16) Haymore, B. L.; Hughes, M.; Mason, J.; Richards, R. L. *J. Chem. Soc., Dalton Trans.* **1988**, 2935.
- (17) Dilworth, J. R.; Kan, C. T.; Richards, R. L.; Mason, J.; Stenhouse, I. A. *J. Organomet. Chem.* **1980**, *201*, C24.

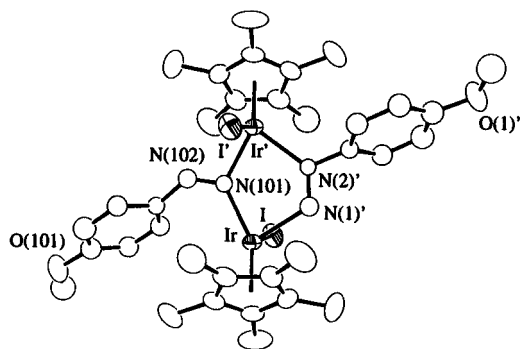
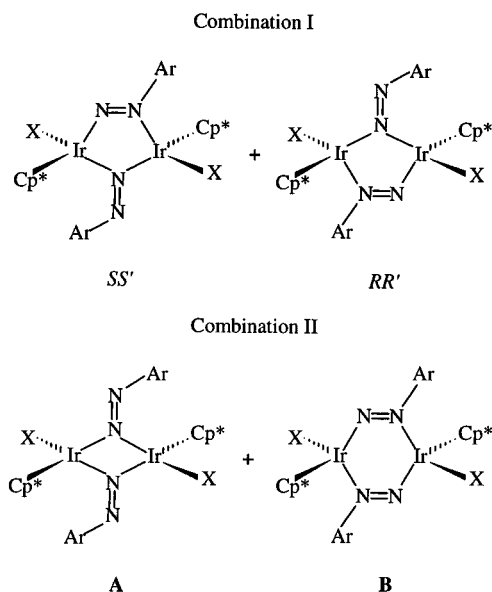


Figure 1. Perspective view of **2** showing the selected atom-numbering scheme. Non-hydrogen atoms are represented by Gaussian ellipsoids at the 50% probability level. Hydrogen atoms are not shown.

Chart 2. Two Possible Combinations for the Disorder Observed in **2**



one kind of molecule, in which both $\mu\text{-}\eta^1$ (**IV**; Chart 1) and $\mu\text{-}\eta^2$ (**V**; Chart 1) bonding modes occur. This molecule is chiral, but there is disorder of two enantiomers in the orientations shown in Chart 2. Combination II accounts for the disorder in terms of equal populations of two *different* centrosymmetric molecules, in which only $\mu\text{-}\eta^1$ (**IV**; Chart 1) and $\mu\text{-}\eta^2$ (**V**; Chart 1) modes occur respectively, as shown.

Combination II is immediately ruled out because, to account for the observed N_α position, the nonbonding $N_\alpha \cdots N_\alpha'$ distance in the molecule with two $\mu\text{-}\eta^1$ modes would be only *ca.* 1.9 Å, significantly shorter than the sum of van der Waals radii for nitrogen (*ca.* 3.0 Å). Therefore, it was concluded that this crystallographic internal disorder was best described by combination I, and the molecule contains two coordinatively different bridging aryldiazenido ligands.

A perspective view of the molecular structure of **2** and the numbering scheme are shown in Figure 1, while the pertinent intramolecular bond lengths and angles are listed in Table 2. There are no unusual intermolecular distances in the crystal structure. Each iridium atom has a distorted three-legged piano-stool coordination environment, provided by the centroid of an $\eta^5\text{-Cp}^*$ ligand, an iodide ligand, and two different coordinated aryldiazenido ligands. The pronounced lengthening of the iridium–iridium separation of 3.5829(7) Å in **2** relative to $[\{\text{Cp}^*\text{Ir}(\text{CO})\}_2(\mu\text{-}\eta^2\text{-}p\text{-N}_2\text{C}_6\text{H}_4\text{OME})][\text{BF}_4]$ (**6**)^{4b} and $[\text{Cp}^*(\text{CO})_2\text{Ir}-\text{Ir}(\text{CO})(\text{Cl})\text{Cp}^*][\text{BF}_4]$ ¹⁰ where the Ir–Ir single-bond distances are 2.723(4) and 2.8266(6) Å, respectively, clearly indicates the

Table 2. Selected Intramolecular Distances (Å) and Angles (deg) for **2**

Bond Distances			
Ir–I	2.6913(8)	Ir–C(10)	2.177(5)
Ir–C(20)	2.154(5)	Ir–C(30)	2.161(5)
Ir–C(40)	2.237(5)	Ir–C(50)	2.249(5)
Ir–Cp ^{*a}	1.820	Ir ^b –N(1)	2.143(9)
Ir–N(2) ^c	2.147(6)	Ir–N(101)	2.030(7)
Ir'–N(101)	2.000(7)	N(1)–N(2) ^c	1.23(1)
N(101)–N(102) ^c	1.19(1)		
Bond Angles			
N(1)'–Ir–I	85.6(2)	N(2)–Ir–I	89.4(2)
N(101)–Ir–I	90.5(2)	N(101)'–Ir–I	87.0(2)
N(101)–Ir–N(1)'	85.0(3)	N(101)'–Ir–N(2)	83.5(3)
N(1)'–Ir–Cp ^{*a}	124.1	N(2)–Ir–Cp ^{*a}	125.1
N(101)–Ir–Cp ^{*a}	141.4	N(101)'–Ir–Cp ^{*a}	133.5
N(2)–N(1)–Ir'	120.3(6)	N(1)–N(2)–Ir	125.5(6)
C(1)–N(2)–Ir	122.4(5)	C(1)–N(2)–N(1)	111.7(7)
Ir–N(101)–Ir'	124.9(4)	N(102)–N(101)–Ir	123.8(6)
N(102)–N(101)–Ir'	110.9(6)	C(101)–N(102)–N(101)	131.7(8)
Ir–N(101)–Ir'	124.9(4)	N(102)–N(101)–Ir	123.8(6)
N(102)–N(101)–Ir'	110.9(6)	C(101)–N(102)–N(101)	131.7(8)

^a Cp* denotes the center of mass of the five Cp* ring carbon atoms.

^b The primed atom labels indicate positions related to those in the table of coordinates by (1 – x, –y, –z). ^c Atoms directly involved in restraints.

absence of a direct metal–metal bond in **2**. Notably, even longer nonbonding Ir^{••}Ir distances have been found in $(\text{Cp}^*\text{IrX}_2)_2$ (X = Cl, 3.7169(1) Å; X = Br, 3.902(13) Å; X = I, 4.072(1) Å).¹⁸ The distance from iridium to the centroid of the Cp* ring is 1.820 Å for **2**, which is shorter than that found in the Ir(I) compound $[\text{Cp}^*\text{Ir}(\text{CO})_2]$ (Ir–Cp* centroid = 1.901 Å)¹⁹ but longer than those in the Ir(III) compounds $(\text{Cp}^*\text{IrX}_2)_2$ (X = Cl, 1.756 Å; X = Br, 1.771 Å; X = I, 1.801 Å).¹⁸ This distance is sensitive to the electron population in the LUMO of a Cp*Ir^{III} fragment (or HOMO of the Cp*Ir^I fragment) because this orbital is metal–Cp* antibonding. The variation of this distance in the above compounds indicates that the LUMO of the Cp*Ir^{III} fragment in **2** has been largely populated and is consistent with the idea that the $\text{N}_2\text{C}_6\text{H}_4\text{OME}^-$ ligand has a stronger electron-donating ability than halides. The Ir–I bond length of 2.6913(8) Å is comparable to the value of 2.694(1) Å found for the terminal Ir–I bond in $(\text{Cp}^*\text{IrI}_2)_2$.^{18b}

An interesting feature of **2** is that the bridging ligand core, consisting of the two iridium atoms, the four nitrogens, and the two *ipso* carbons of the aryl rings, is essentially planar, with only small deviations from the best least-squares plane defined by the planar Ir'–N(1)–N(2)–Ir–N(101)' ring.²⁰ This planarity suggests a degree of π -electron delocalization over the five-membered ring and N(102)'.²⁰

For the $\mu\text{-}\eta^2$ -bridging aryldiazenido ligand, the N(1)–N(2) bond length is 1.23(1) Å, consistent with a N=N double bond. This value is comparable to that found in $(\mu\text{-H})\text{Os}_3(\text{CO})_{10}(\mu\text{-}\eta^2\text{-N}_2\text{Ph})$ (N–N = 1.233(2) Å)^{7a} and is slightly smaller than that found in $[\{\text{Cp}^*\text{Ir}(\text{CO})\}_2(\mu\text{-}\eta^2\text{-}p\text{-N}_2\text{C}_6\text{H}_4\text{OME})][\text{BF}_4]$ (**6**) (N–N = 1.29(2) Å).^{4b} The N=N group is symmetrically bridging between the two iridium centers with Ir(1)–N(1) = 2.143(9) Å and Ir(2)–N(2) = 2.147(6) Å. These distances are possibly longer than those found in $[\{\text{Cp}^*\text{Ir}(\text{CO})\}_2(\mu\text{-}\eta^2\text{-}p\text{-}$

(18) (a) Churchill, M. R.; Julis, S. A. *Inorg. Chem.* **1977**, *16*, 1488. (b) Churchill, M. R.; Julis, S. A. *Inorg. Chem.* **1979**, *18*, 1215.

(19) Ball, R. G.; Graham, W. A. G.; Heinekey, D. M.; Hoyano, J. K.; McMaster, A. D.; Mattson, B. M.; Michel, S. T. *Inorg. Chem.* **1990**, *29*, 2013.

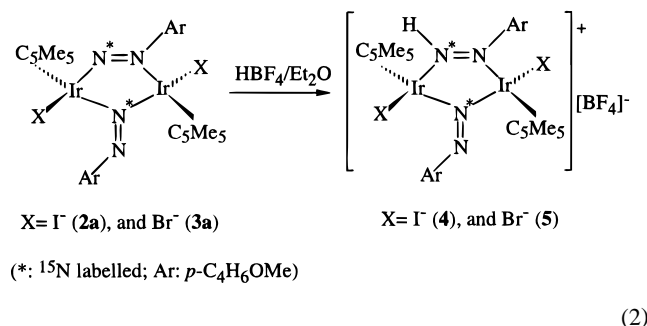
(20) The five-membered ring Ir', N(1), N(2), Ir, and N(101)' is essentially planar. Deviations from the best least-squares plane through these atoms: N(1), –0.074(11) Å; N(2), 0.056(9) Å; N(101)', 0.028(8) Å; C(1), 0.085(12) Å; N(102)', 0.191(11) Å; C(101)', –0.003(13) Å.

$\text{N}_2\text{C}_6\text{H}_4\text{OMe}\}\{\text{BF}_4\}$ (**6**) ($\text{Ir}(1)-\text{N}(1) = 2.02(2)$ Å and $\text{Ir}(2)-\text{N}(2) = 2.06(2)$ Å).^{4b}

For the μ - η^1 -bridging aryldiazenido ligand, the $\text{N}(101)-\text{N}(102)$ distance of 1.19(1) Å is comparable with those found in similarly coordinated aryldiazenido complexes.^{7b-g} This bridge is also essentially symmetrical ($\text{Ir}(1)-\text{N}(101) = 2.030(7)$ Å, $\text{Ir}(2)-\text{N}(101) = 2.000(7)$ Å, and $\text{Ir}-\text{N}(\text{average}) = 2.015(10)$ Å) and involves an angle of $\text{Ir}(1)-\text{N}(101)-\text{Ir}(2) = 124.9(4)^\circ$. This angle, however, is significantly larger than that in a similar coordinated aryldiazenido compound $\{[\text{Ir}(\text{NO})(\text{PPh}_3)_2(\mu\text{-O})(\mu\text{-}\eta^1\text{-}o\text{-N}_2\text{C}_6\text{H}_4\text{NO}_2)]\{\text{PF}_6\}$ ($\text{Ir}-\text{N}-\text{Ir}' = 94(4)^\circ$).^{7b}

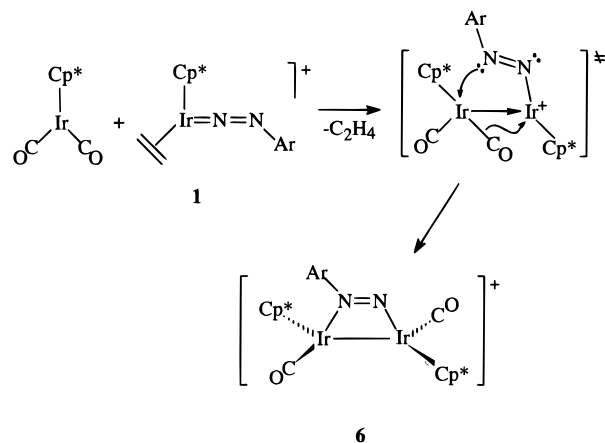
Another feature of the bridging aryldiazenido ligands is that the planes of the aromatic rings of the *p*-methoxyphenyl groups each make an angle *ca.* 120° with the molecular core plane. This feature indicates nonconjugation of the π electrons between the $\text{N}=\text{N}$ group and its aromatic ring in both of the bridging aryldiazenido ligands. A similar phenomenon has also been observed in other bridging aryldiazenido complexes.⁷

Protonation of $[\text{Cp}^*\text{IrX}]_2(\mu\text{-}\eta^2\text{-}p\text{-}^{15}\text{N}_\alpha\text{NC}_6\text{H}_4\text{OMe})(\mu\text{-}\eta^1\text{-}p\text{-}^{15}\text{N}_\alpha\text{NC}_6\text{H}_4\text{OMe})$, ($\text{X} = \text{I}$ (2a**), Br (**3a**)).** Protonation of **2a** or **3a** in CDCl_3 with a slight excess of $\text{HBF}_4/\text{Et}_2\text{O}$ changes the color of the solution immediately to dark brown, accompanied by the formation of a precipitate in either case. The NMR studies of these protonated species, carried out *in situ* for **2a** and after isolation of the precipitate for **3a**, indicate they are the singly protonated products **4** and **5**, respectively (eq 2).



Compound **4** shows a clean ^{15}N NMR spectrum consisting of two peaks, a sharp singlet at δ 65.1, which is in a position almost identical to that for **2a** (δ 64.1), and the other, a broad resonance at δ -110.7. Importantly, the resonance near δ 300 for the precursor **2a** disappeared. This clearly indicates that protonation of **2a** has occurred at the $^{15}\text{N}_\alpha$ nucleus of the μ - η^2 -coordinated aryldiazenido ligand (**V**; Chart 1), as shown in eq 2. The sensitivity of the ^{15}N chemical shift to the presence of a lone pair of electrons on the $^{15}\text{N}_\alpha$ nucleus in aryldiazenido ligands has been mentioned above.^{16,17} Formation a μ - η^2 -coordinated aryldiazene ligand due to the protonation at the $^{15}\text{N}_\alpha$ nucleus in question decreases the deshielding effect at this nucleus and readily accounts for the shift to higher field, i.e., to δ -110.7. A similar upfield shift was observed upon a protonation of N_α in $(\mu\text{-H})\text{Os}_3(\text{CO})_{10}(\mu\text{-}\eta^2\text{-}p\text{-N}_2\text{C}_6\text{H}_4\text{Me})$, where the $^{15}\text{N}_\alpha$ resonance moved from δ 313 to δ -61.^{7a} Furthermore, the almost identical resonances observed at δ 65.1 for **4** and δ 64.1 for **2a** suggest that the μ - η^1 -coordinated aryldiazenido ligand remains intact. The ^1H NMR spectrum of the same sample showed, in addition to the resonances for the Cp^* and $\text{C}_6\text{H}_4\text{OMe}$ groups, a sharp doublet at δ 15.2 with $J^{15}\text{NH} = 79$ Hz, which is undoubtedly assigned to $\text{H}-^{15}\text{N}_\alpha$. The $J^{15}\text{NH}$ coupling observed in the ^1H NMR spectrum was not resolved in the ^{15}N NMR spectrum. A similar ^1H NMR spectrum was observed for the formation of **5** by protonating **3a**, the $\text{H}-^{15}\text{N}_\alpha$ resonance of the η^2 -coordinated aryldiazene ligand occurring

Scheme 1. Possible Formation Mechanism of **6**



at δ 15.3 with $J^{15}\text{NH} = 79$ Hz. No resonance was evident in either case for protonation at N_β of the μ - η^1 - aryldiazenido ligand. This is consistent with the ^{15}N NMR analysis, and we conclude that protonation occurred only at the α -nitrogen of the η^2 -coordinated bridging aryldiazenido ligand. Samkoff and co-workers reported a similar feature for their two isomeric complexes $(\mu\text{-H})\text{Os}_3(\text{CO})_{10}(\mu\text{-}\eta^2\text{-}p\text{-N}_2\text{C}_6\text{H}_4\text{Me})$ and $(\mu\text{-H})\text{Os}_3(\text{CO})_{10}(\mu\text{-}\eta^1\text{-}p\text{-N}_2\text{C}_6\text{H}_4\text{Me})$, where only the μ - η^2 -bridging aryldiazenido isomer could be protonated and formed a similarly coordinated aryldiazene compound, even with a large excess of $\text{HBF}_4 \cdot \text{Et}_2\text{O}$.^{7a} This has been reconciled with the similar basicity order ($\text{N}_\alpha > \text{N}_\beta$) observed for mononuclear doubly-bident aryldiazenido complexes.^{7a}

As expected for the proposed structures of **4** and **5**, the two Cp^* ligands are again inequivalent. The chemical shifts of these two Cp^* resonances (δ 1.62, 2.00 for **4**; δ 1.51, 1.90 for **5**) are both significantly shifted downfield from those observed for their precursors **2** and **3** (δ 1.29, 1.37 for **2**; δ 1.22, 1.28 for **3**). As the protonation is established to occur only at the α -nitrogen of the η^2 -coordinated aryldiazenido ligand (but not at N_β of the η^2 -coordinated one), this parallel shift of *both* Cp^* signals in either **2** or **3** upon protonation convincingly removes the possibility that **2** or **3** may exist *in solution* as a mixture of the two symmetrical isomers **A** and **B** depicted in Chart 2. This leads us to conclude that in solution **2** and **3** have the same structure as that crystallographically determined for **2** in the solid state.

Synthesis and Characterization of $[\{\text{Cp}^*\text{Ir}(\text{CO})\}_2(\mu\text{-}\eta^2\text{-}p\text{-N}_2\text{C}_6\text{H}_4\text{OMe})][\text{BF}_4]$ (6**).** Various electron-rich transition metal complexes have been used as ligands in preparation of dinuclear or multinuclear complexes.²¹ Since $\text{Cp}^*\text{Ir}(\text{CO})_2$ is a convenient metal base, its reaction with **1** was carried out in expectation of forming a dinuclear complex. Treatment of equimolar amounts of $\text{Cp}^*\text{Ir}(\text{CO})_2$ and compound **1** in EtOH under reflux afforded the dinuclear complex **6**. Recrystallization

- (21) (a) Einstein, F. W. B.; Yan, X.; Zhang, X.; Sutton, D. J. *Organomet. Chem.* **1992**, 439, 221. (b) Green, M.; Mills, R. M.; Pain, G. N.; Stone, F. G. A.; Woodward, P. *J. Chem. Soc., Dalton Trans.* **1982**, 1309. (c) Nutton, A.; Maitlis, P. M. *J. Organomet. Chem.* **1979**, 166, C21. (d) Aldridge, M. L.; Green, M.; Howard, J. A. K.; Pain, G. N.; Porter, S. J.; Stone, F. G. A.; Woodward, P. *J. Chem. Soc., Dalton Trans.* **1982**, 1333. (e) Leonard, K.; Werner, H. *Angew. Chem., Int. Ed. Engl.* **1977**, 16, 649. (f) Del Paggio, A. A.; Muettterties, E. L.; Heinekey, D. M.; Day, V. W.; Day, C. S. *Organometallics* **1986**, 5, 575. (g) Einstein, F. W. B.; Jones, T.; Pomeroy, R. K.; Rushman, P. *J. Am. Chem. Soc.* **1984**, 106, 2707. (h) Einstein, F. W. B.; Pomeroy, R. K.; Rushman, P.; Willis, A. C. *Organometallics* **1985**, 4, 250. (i) Green, M.; Hankey, D. R.; Howard, J. A. K.; Louca, P.; Stone, F. G. A. *J. Chem. Soc., Chem. Commun.* **1983**, 757. (j) Freeman, M. J.; Miles, A. D.; Murray, M.; Orpen, A. G.; Stone, F. G. A. *Polyhedron* **1984**, 3, 1093.

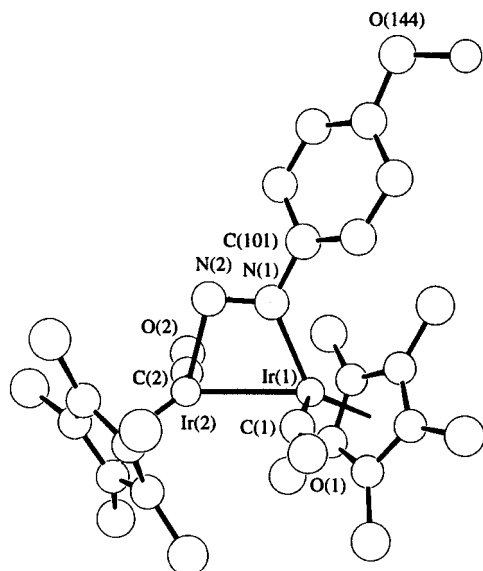


Figure 2. Perspective view of the cation of **6** showing the selected atom-numbering scheme. Hydrogen atoms are not shown.

of **6** from acetone and hexanes gave crystals suitable for X-ray crystallographic analysis.

In this reaction, formation of a doubly-bent aryldiazenido intermediate upon replacing the ethylene in **1** by the metal base $\text{Cp}^*\text{Ir}(\text{CO})_2$ is presumed (Scheme 1), which is analogous to the intermediate proposed to be formed when I^- and Br^- are used (see general discussion below). This intermediate then is proposed to rearrange rapidly by a pathway involving a terminal-bridging-terminal transfer of a CO group assisted by bridging of the $\text{N}_2\text{C}_6\text{H}_4\text{OMe}$ ligand to give product **6**. Support for this suggestion can be found in the related compound $[\text{Cp}^*(\text{CO})_2\text{Ir} \rightarrow \text{Ir}(\text{CO})(\text{Cl})\text{Cp}^*][\text{BF}_4]$,¹⁰ which is synthesized by Ag^+ -mediated displacement of one Cl^- ligand from $\text{Cp}^*\text{Ir}(\text{CO})\text{Cl}_2$ by the metal base $\text{Cp}^*\text{Ir}(\text{CO})_2$. Furthermore, the CO groups in $[\text{Cp}^*(\text{CO})_2\text{Ir} \rightarrow \text{Ir}(\text{CO})(\text{Cl})\text{Cp}^*][\text{BF}_4]$ undergo fast exchange at room temperature, presumably by a terminal-bridging interchange mechanism, which closely parallels the mechanism suggested for the formation of **6**.²²

Unlike the bridging aryldiazenido complexes **2** and **3**, compound **6** is air-sensitive both in solution and in the solid state. The infrared spectrum of **6** exhibits the expected two $\nu(\text{CO})$ bands at 1922 and 1970 cm^{-1} for the two terminal CO ligands. However, the $\nu(\text{NN})$ absorption could not be unambiguously assigned possibly because of overlap with other IR-active bands in the fingerprint region. The mass spectrum (FAB) reveals the dinuclear nature of **6** by exhibiting an isotopic pattern for the cation that agrees with the simulated pattern, as well as other related fragments. The ambient temperature ^1H NMR spectrum of **6** in CDCl_3 shows the expected resonances for *one* $\text{C}_6\text{H}_4\text{OMe}$ group and *two* different Cp^* resonances at δ 2.13 and 2.01, respectively.

X-ray Structure of $[\{\text{Cp}^*\text{Ir}(\text{CO})\}_2(\mu\text{-}\eta^2\text{-}p\text{-}\text{N}_2\text{C}_6\text{H}_4\text{OMe})][\text{BF}_4]$ (6**).** The single-crystal X-ray crystallographic analysis of $[\{\text{Cp}^*\text{Ir}(\text{CO})\}_2(\mu\text{-}\eta^2\text{-}p\text{-}\text{N}_2\text{C}_6\text{H}_4\text{OMe})][\text{BF}_4]$ (**6**) established the dinuclear nature of the cation in this complex. As shown in Figure 2, the cation of **6** contains two iridium atoms bridged by a $\mu\text{-}\eta^2$ -coordinated aryldiazenido ligand, and each of these iridium atoms is also linked to a terminal carbonyl and an η^5 -pentamethylcyclopentadienyl ligand. The pertinent intramolecular dimensions for **6** are listed in Table 3.

Table 3. Selected Bond Lengths (Å) and Interbond Angles (deg) of **6**^a

Bond Lengths			
Ir(1)–Ir(2)	2.723(4)	Ir(1)–N(1)	2.02(2)
Ir(1)–C(1)	1.81(2)	Ir(1)–C(10)	2.26(2)
Ir(1)–C(11)	2.27(2)	Ir(1)–C(12)	2.24(2)
Ir(1)–C(13)	2.26(2)	Ir(1)–C(14)	2.26(2)
Ir(2)–N(2)	2.06(2)	Ir(2)–C(2)	1.79(2)
Ir(2)–C(20)	2.26(2)	Ir(2)–C(21)	2.27(2)
Ir(2)–C(22)	2.26(2)	Ir(2)–C(23)	2.28(2)
Ir(2)–C(24)	2.25(2)	N(1)–N(2)	1.29(2)
N(1)–C(101)	1.41(3)	C(1)–O(1)	1.21(2)
C(2)–O(2)	1.20(2)	O(144)–C(104)	1.41(4)
O(144)–C(144)	1.41(6)	Ir(3)–Ir(4)	2.719(4)
Ir(3)–N(3)	2.04(2)	Ir(3)–C(3)	1.80(2)
Ir(3)–C(30)	2.27(2)	Ir(3)–C(31)	2.27(2)
Ir(3)–C(32)	2.25(2)	Ir(3)–C(33)	2.26(2)
Ir(3)–C(34)	2.26(2)	N(3)–N(4)	1.30(2)
N(3)–C(201)	1.39(3)	C(3)–O(3)	1.20(2)
Ir(4)–N(4)	2.08(2)	Ir(4)–C(4)	1.81(2)
Ir(4)–C(40)	2.26(2)	Ir(4)–C(41)	2.25(2)
Ir(4)–C(42)	2.25(2)	Ir(4)–C(43)	2.26(2)
Ir(4)–C(44)	2.25(2)	C(4)–O(4)	1.20(2)
O(244)–C(204)	1.40(4)	O(244)–C(244)	1.50(7)

Bond Angles			
Ir(2)–Ir(1)–N(1)	68.0(10)	Ir(4)–Ir(3)–N(3)	68.8(10)
Ir(2)–Ir(1)–C(1)	84.8(19)	Ir(4)–Ir(3)–C(3)	91.4(19)
N(1)–Ir(1)–C(1)	94.0(16)	N(3)–Ir(3)–C(3)	90.4(18)
Ir(1)–N(1)–N(2)	115.1(25)	Ir(3)–N(3)–N(4)	114.0(23)
Ir(1)–N(1)–C(101)	130.0(20)	Ir(3)–N(3)–C(201)	130.7(23)
N(2)–N(1)–C(101)	114.9(24)	N(4)–N(3)–C(201)	115.3(23)
Ir(1)–C(1)–O(1)	162.9(51)	Ir(3)–C(3)–O(3)	176.0(53)
Ir(1)–Ir(2)–N(2)	70.7(10)	Ir(3)–Ir(4)–N(4)	70.9(10)
Ir(1)–Ir(2)–C(2)	91.4(24)	Ir(3)–Ir(4)–C(4)	91.0(24)
N(2)–Ir(2)–C(2)	94.2(22)	N(4)–Ir(4)–C(4)	89.6(21)
Ir(2)–N(2)–N(1)	106.2(24)	Ir(4)–N(4)–N(3)	106.3(23)
Ir(2)–C(2)–O(2)	170.3(49)	Ir(4)–C(4)–O(4)	171.1(62)
C(144)–O(144)–C(104)	112.9(41)	C(244)–O(244)–C(204)	122.0(41)

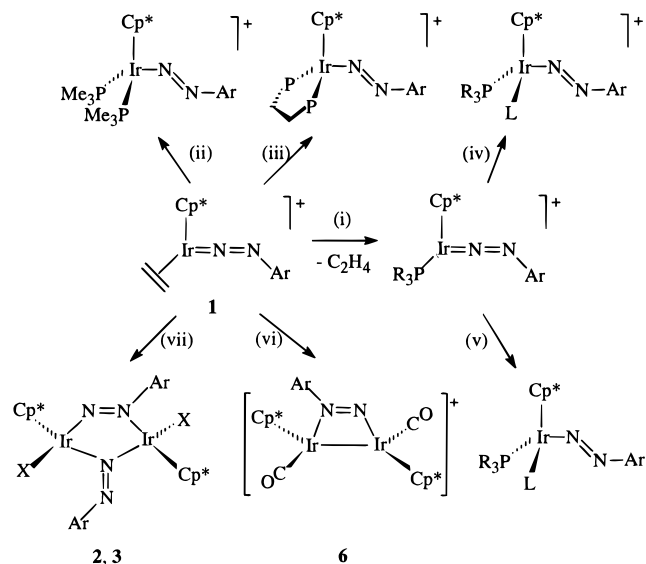
^a Atomic sites with 85% occupancy listed only.

The Ir(1)–Ir(2) distance of 2.723 (4) Å is significantly shorter than the $\text{Ir}\cdots\text{Ir}$ distance of 3.5829(7) Å in the related bridging aryldiazenido complex **2**, in which the two iridium atoms are considered as nonbonding. The two iridium atoms in **6** are considered to be directly bonded to each other by a single bond in order to fulfill the 18-electron requirement. Interestingly, this Ir–Ir bond distance is also significantly shorter (by *ca.* 0.11 Å) than those found in diiridium complexes that have no supporting bridging ligand, e.g., the Ir–Ir single-bond distance is 2.8266(6) Å for $[\text{Cp}^*(\text{CO})_2\text{Ir} \rightarrow \text{Ir}(\text{CO})(\text{Cl})\text{Cp}^*][\text{BF}_4]$ ^{10,22} and 2.8394(12) Å for $[\text{Cp}^*(\text{CO})_2\text{Ir} \rightarrow \text{Ir}(\text{CO})_2\text{Cp}^*][\text{BF}_4]$.²³ This clearly shows the shortening effect that the bridging aryldiazenido ligand has on the Ir–Ir bond length.

By sharing the bridging aryldiazenido ligand and the Ir–Ir single bond, each of the iridium atoms is approximately in a distorted three-legged piano stool coordination environment, with the legs separated at angles Ir(2)–Ir(1)–N(1) = 68.0(10)°, Ir(2)–Ir(1)–C(1) = 84.8(19)°, and C(1)–Ir(1)–N(1) = 94.0(16)° for the Ir(1) atom and Ir(1)–Ir(2)–N(2) = 70.7(10)°, Ir(1)–Ir(2)–C(2) = 91.4(24)°, and C(2)–Ir(2)–N(2) = 94.2(22)° for the Ir(2) atom. The significantly smaller Ir–Ir–N angles, by comparison with other bond angles at the both iridium atoms, may reflect the highly strained four-membered ring formed by the two iridium atoms and the two nitrogen atoms. These values are, in fact, similar to those found in the related complex $(\mu\text{-H})\text{Os}_3(\text{CO})_{10}(\mu\text{-}\eta^2\text{-N}_2\text{Ph})$, in which the corresponding angles are 64.4(7) and 68.6(7)°. ^{7a}

(22) Yan, X.; Batchelor, R. J.; Einstein, F. W. B.; Zhang, X.; Nagelkerke, R.; Sutton, D. Submitted to *Inorg. Chem.*

(23) Einstein, F. W. B.; Jones, R. H.; Zhang, X.; Yan, X.; Nagelkerke, R.; Sutton, D. *J. Chem. Soc., Chem. Commun.* **1989**, 1424.

Scheme 2^a

^a Reagents used: (i) PR_3 (R = Ph, *p*-tol); (ii) PMe_3 ; (iii) diphos = $(\text{Ph}_2\text{P}(\text{CH}_2)_2\text{PPh}_2)$; (iv) R = Ph, L = CO, PMe_3 ; R = *p*-tol, L = PMe_3 ; (v) R = Ph, L = CN^- , H^- ; (vi) $\text{Cp}^*\text{Ir}(\text{CO})_2$; (vii) X = I^- (**2**), Br^- (**3**).

The pentamethylcyclopentadienyl ligands in **6** contain no peculiarities in bond lengths or bond angles. Likewise, there are no significant differences in the ring carbon to iridium bond lengths, indicating the Cp^* ligands are symmetrically coordinated to the iridium atoms.

The nitrogen–nitrogen bond of the aryldiazenido ligand is essentially coplanar with the iridium–iridium bond, with $\text{Ir}(1)\text{--N}(1) = 2.02(2) \text{ \AA}$ and $\text{Ir}(2)\text{--N}(2) = 2.06(2) \text{ \AA}$. The $\text{N}(1)\text{--N}(2)$ bond length ($1.29(2) \text{ \AA}$) has the expected value for an $\text{N}=\text{N}$ double-bond distance but is perhaps slightly longer than found in other bridged aryldiazenido complexes. For example, $\text{N}=\text{N}$ double-bond lengths of $1.20(4)$ and $1.23(1) \text{ \AA}$ were found for $\mu\text{-}\eta^2\text{-aryldiazenido}$ ligands, separately, in $(\mu\text{-H})\text{Os}_3(\text{CO})_{10}(\mu\text{-}\eta^2\text{-N}_2\text{Ph})$ ^{7a} and compound **2** (vide supra). As in complex **2** and other bridging aryldiazenido complexes, the NN group of the diazenido ligand is not coplanar with its aromatic ring, indicating lack of conjugation of π electrons between these two functional groups.

General Comments

In this and previous work, the singly-bent aryldiazenido complex $[\text{Cp}^*\text{Ir}(\text{C}_2\text{H}_4)(p\text{-N}_2\text{C}_6\text{H}_4\text{OMe})][\text{BF}_4]$ (**1**) has proved to be a useful precursor for the syntheses of a series of structurally different aryldiazenido complexes (Scheme 2).^{4,5}

From the reactions in Scheme 2, it seems evident that, as expected, substituting the ethylene group in $[\text{Cp}^*\text{Ir}(\text{C}_2\text{H}_4)(p\text{-N}_2\text{C}_6\text{H}_4\text{OMe})][\text{BF}_4]$ by another ligand is the most probable initial step involved in all these reactions. This substitution indeed occurs rather readily due to the lability of the ethylene ligand induced by the strong π back-bonding from Ir to the strong π -acid (singly-bent aryldiazenido) ligand.^{4a} The most fascinating feature in Scheme 2 is the structural diversity of the products. When the entering ligand L is a weak π -acid, such as PPh_3 and $\text{P}(p\text{-tol})_3$ in reactions i of Scheme 2, the aryldiazenido ligand in the product cation $[\text{Cp}^*\text{Ir}(\text{L})(p\text{-N}_2\text{C}_6\text{H}_4\text{OMe})]^+$ prefers to adopt a singly-bent geometry, as it does in **1** itself, where C_2H_4 is also a weak π -acid. The expected conformational structure, fluxionality, and properties of the singly-bent aryldiazenido ligand in these complexes have been rationalized in terms of the orbital interactions of the singly-bent N_2Ar ligand with the fragment Cp^*IrL and have shown excellent consistency with experimental observations.^{4a,5}

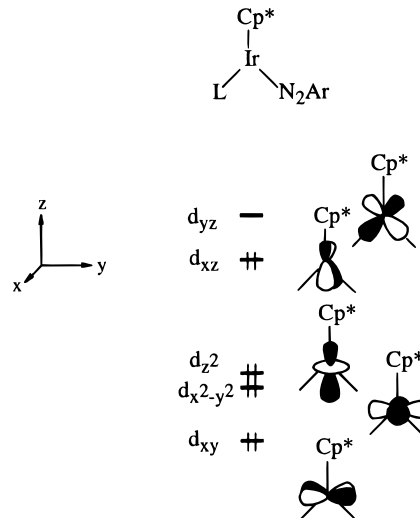
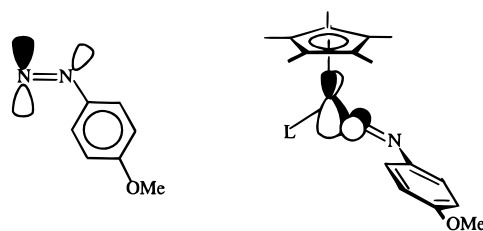
Chart 3. Frontier Orbitals for $[\text{Cp}^*\text{Ir}(\text{L})(\text{N}_2\text{Ar})]^+$ 

Chart 4



(a) LUMO of $[p\text{-N}_2\text{C}_4\text{H}_6\text{OMe}]^+$ (b) π interaction between Cp^*IrL as a singly-bent ligand and $[p\text{-N}_2\text{C}_4\text{H}_6\text{OMe}]^+$

However, when the entering ligand is a π -base, as in reactions vii with $\text{X}^- = \text{I}^-$ and Br^- , the products contain bridging aryldiazenido ligands. Since the steric effect between L (or X) and the aryldiazenido ligand in the uncrowded two-legged piano stool complexes $[\text{Cp}^*\text{Ir}(\text{L})(p\text{-N}_2\text{C}_6\text{H}_4\text{OMe})]^+$ or $[\text{Cp}^*\text{IrX}(p\text{-N}_2\text{C}_6\text{H}_4\text{OMe})]$ resulting from the initial substitution would be small, the importance of the electronic nature of the ancillary ligands L or X^- in determining the structures of the products is evident. In the following discussion, similar fragment orbital interaction arguments will be used to discuss the electronic interactions that should occur in the proposed key intermediate $\text{Cp}^*\text{IrX}(p\text{-N}_2\text{C}_6\text{H}_4\text{OMe})$. The reaction of **1** with $\text{Cp}^*\text{Ir}(\text{CO})_2$ ((vi), Scheme 2) can be rationalized in a similar fashion.

The frontier orbitals of the Cp^*M fragment have been given elsewhere.²⁴ From this, the frontier orbitals for the two-legged piano stool molecule $[\text{Cp}^*\text{Ir}(\text{L})(p\text{-N}_2\text{C}_6\text{H}_4\text{OMe})]^+$ can be readily developed and are shown in Chart 3, where only σ interactions between Cp^*Ir and the two ligands are considered. The HOMO of this molecule is the d_{xz} orbital in the chosen coordinate system, and L and the nitrogens of the aryldiazenido ligand are in the yz plane. As has been pointed out previously,^{4a} the LUMO of the singly-bent aryldiazenido ligand is of π character and is located in the plane of the bent aryldiazenido ligand, as shown in Chart 4a. If, for the present, any π orbitals of the ancillary ligand L are ignored, the primary π interaction is clearly the back-bonding interaction between the HOMO (d_{xz}) of Cp^*Ir and LUMO of the aryldiazenido ligand as shown in Chart 4 (b). This is because the HOMO of the metal fragment is antibonding between iridium and the Cp^* ligand and the

(24) (a) Albright, T. A.; Burdett, J. K.; Whangbo, M.-H. *Orbital Interactions in Chemistry*; John Wiley & Sons: New York, 1985. (b) Albright, T. A. *Tetrahedron* **1982**, *38*, 1339.

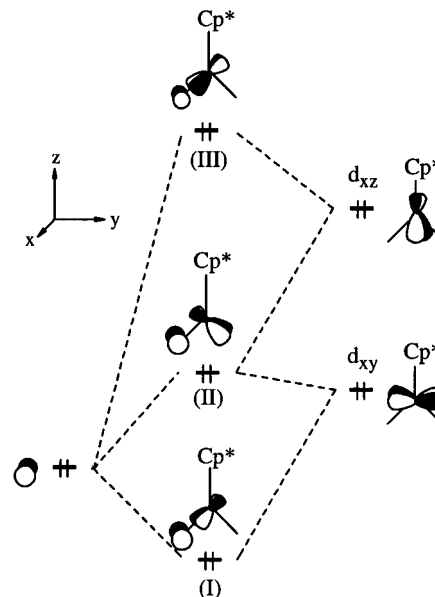
LUMO of the aryldiazenido ligand is a very low-lying empty orbital, even lower than that of the NO^+ ligand.^{4a} It should be further noted that, though the lower energy orbital d_{xy} can also interact with LUMO of the N_2Ar^+ ligand, it will participate in π bonding to a lesser extent due to its lower energy, and hence its effect can be considered of secondary importance.

The principal issue now remaining is to determine the π -electronic influence of the different ancillary ligands L on these π interactions between the Cp^*Ir fragment and the $\text{N}_2\text{-Ar}^+$ ligand. When L is a π -acid, it will be expected to compete with the N_2Ar^+ ligand for the electrons in the d_{xz} orbital, i.e., the HOMO. If L is only a weak π -acid, the π back-bonding from the Cp^*Ir fragment to the N_2Ar^+ ligand, known to be a strong π -acid,^{4a} would be expected to be perturbed rather little. In agreement, the molecular structure of $[\text{Cp}^*\text{Ir}(\text{L})(p\text{-N}_2\text{C}_6\text{H}_4\text{OMe})]^+$, where L is the weak π -acid C_2H_4 or $\text{P}(p\text{-tol})_3$, does indeed have the plane containing the N_2Ar group (and hence the LUMO of this ligand) positioned perpendicular to the plane defined by the centroid of Cp^* , Ir, and N_α atoms as depicted in Chart 4 (b). As the π -acidity of the ancillary ligand is increased, a decrease in the effectiveness of this π back-bonding from Cp^*Ir to N_2Ar^+ will be expected. This is evidenced by the observed decrease of $\nu(\text{NN})$ absorptions of the singly-bent aryldiazenido ligand with the relative increase of the π -acidity of L = ethylene or phosphine in these same complexes $[\text{Cp}^*\text{Ir}(\text{L})(p\text{-N}_2\text{C}_6\text{H}_4\text{OMe})]^+$; for instance, $\nu(\text{NN})$ absorptions at 1709 and 1701 cm^{-1} observed in EtOH solution for L = $\text{P}(p\text{-tol})_3$ and PPh_3 , respectively, are lower than that of its ethylene analogue **1**, which has $\nu(\text{NN})$ at 1724 cm^{-1} in the same solvent.^{4a,5} A similar trend has also been observed from the ^{15}N NMR spectra in that the more deshielded $^{15}\text{N}_\alpha$ resonances of δ 33.7 and 33.2 for L = $\text{P}(p\text{-tol})_3$ and PPh_3 , respectively, compared with δ -2.26 for **1** are indicative of less π back-bonding experienced by the singly-bent aryldiazenido ligand in **1**.^{4a,5} These are consistent with the general view that C_2H_4 is a better π -acid than the PR_3 ligand. Ultimately, if the ancillary ligand were a strong π -acid, by delocalizing a large degree of π -electron density from the metal-centered HOMO into its accepting orbital, it would severely weaken the π back-bonding from the metal fragment Cp^*Ir to the N_2Ar^+ ligand and probably labilize this ligand to dissociate as the free aryldiazonium ion. This may account for the experimental fact that, despite numerous synthetic strategies and routes, we have had no success in obtaining either $[\text{Cp}^*\text{Ir}(\text{CO})(p\text{-N}_2\text{C}_6\text{H}_4\text{OMe})][\text{BF}_4]$ or $\text{Cp}^*\text{Ir}(\text{CN})(p\text{-N}_2\text{C}_6\text{H}_4\text{OMe})$.¹⁰ For example, the former complex is not obtained when **1** is reacted with CO or when $\text{Cp}^*\text{Ir}(\text{CO})_2$ is reacted with $[p\text{-N}_2\text{C}_6\text{H}_4\text{OMe}][\text{BF}_4]$.²²

If the ancillary ligand is a π -base, the orbital interactions between the metal center and its ligands become slightly more complicated. A π -base has at least one filled orbital of π symmetry (i.e., in the direction perpendicular to its coordination direction), and this orbital is lower in energy than the metal-centered ones. When this π -base coordinates to the $\text{Cp}^*\text{IrN}_2\text{-Ar}^+$ fragment in the direction "trans" to the aryldiazenido ligand, one of its filled π orbitals will be of the correct symmetry to interact with the metal-centered d_{xz} and d_{xy} orbitals. Since d_{xz} and d_{xy} are also filled orbitals, ignoring for the moment the LUMO of the aryldiazenido ligand, the π interaction between these filled orbitals is a three-orbital–six-electron one, resulting in orbitals I–III, as shown in Scheme 3.

As a result, the HOMO of Cp^*Ir is now effectively the upper orbital (III) in Scheme 3 and is thus significantly raised in energy. This is because, in addition to the antibonding character of the d_{xz} and ligand π interaction, it has a large antibonding contribution from the energetically more favorable metal d_{xy} –

Scheme 3. π Interaction between Cp^*Ir and L



ligand π interaction. It is also evident that the more π -basic the ligand L is, the more this antibonding contribution will be seen in the HOMO of Cp^*Ir . Normally, taken in isolation, this three-orbital–six-electron interaction would be energetically unfavorable and tend to labilize the ancillary ligand L. This may not be the case when the effect of the above-mentioned strong π -accepting orbital of the singly-bent aryldiazenido ligand is factored in. The increased energy of the Cp^*Ir HOMO would be expected to favor an increase in the π back-bonding to the N_2Ar^+ ligand. However, due to the contribution from the d_{xy} –ligand π interaction, the HOMO depicted as III in Scheme 3 now is not in a geometrically favorable situation to back-bond with the N_2Ar^+ ligand (LUMO). In other words, the HOMO of the metal center and the LUMO of the N_2Ar^+ ligand, while proximate in energy, will have poor overlap due to their essentially orthogonal geometric disposition. Note that the essentially nonbonding orbital d_{xy} , II in Scheme 3, does have a suitable orientation to back-bond to the aryldiazenido ligand, but the larger energy difference between this orbital and the N_2Ar^+ LUMO will not make for an effective interaction. However, it is important to point that it is in this situation where the noncrossing rule²⁵ becomes less valid²⁶ and symmetry-allowed thermal electron transfer becomes most favored. By this electron transfer from the HOMO of Cp^*IrL to the LUMO of the N_2Ar^+ ligand, a 16e species with Ir(III) and a doubly-bent aryldiazenido ligand would result. Concomitant with this electron transfer, the doubly-bent aryldiazenido ligand of this 16e species would most likely reorientate itself by a rotation of 90° along the Ir-N_α single bond. The driving force behind this is that (i) it will orthogonalize the filled metal d_{xy} orbital and the lone-pair orbital at N_α , and hence significantly lower the unfavorable energy caused by the antibonding interaction between them, and (ii) it will stabilize the antibonding interaction between the π -donating orbital of L and the metal d_{xy} orbital by bringing an empty π^* orbital of the N_2Ar ligand into the correct symmetry, which is perpendicular to the plane of the N_2Ar ligand. With this rotation, the molecule changes its

- (25) (a) McWeeney, R. *Coulson's Valence*; Oxford University Press: New York, 1973. (b) Salem, L. *Electrons in Chemical Reactions: First Principles*; Wiley: New York, 1982; Chapters 4 and 5. (c) Woodward, R. B.; Hoffmann, R. *The Conservation of Orbital Symmetry*; Academic Press: New York, 1969.
- (26) Salem, L. *Electrons In Chemical Reactions: First Principles*; Wiley: New York, 1982; p 148.

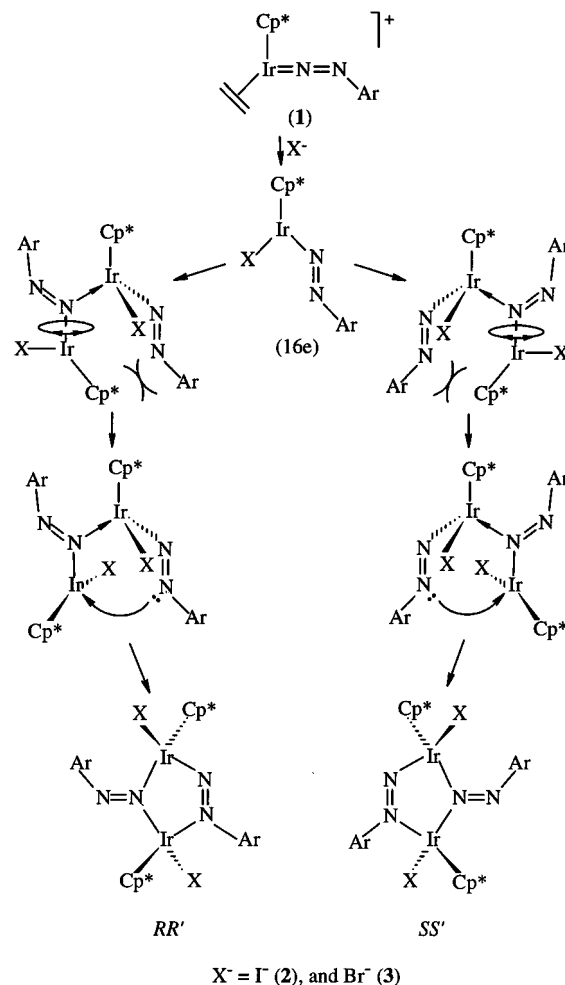
symmetry from an asymmetric, or a chiral, one to one with mirror symmetry where the N_2Ar ligand plane is coincident with the plane defined by the centroid of Cp^* , Ir, and L .²⁷

As mentioned above, the thermal electron transfer in our system can only occur when the π -basicity of the ancillary ligand L involved is *strong enough*. For a weakly π -basic ligand L , the interaction depicted in Scheme 3 will be expected to be weak, which may not be able to prompt the described thermal electron transfer to occur. Conversely, this weak π -base will itself be largely labilized due to the unfavorable six-electron–three-orbital interaction. In practice, reaction of **1** with the weak π -bases Cl^- and RO^- ($R = H, Me, Et$), separately, under conditions similar to those used for preparation of **2** and **3** failed to produce either the dibridging aryldiazenido analogue of **2** and **3** or the singly-bent aryldiazenido analogue of **1**. This is entirely consistent with the logic of the above theoretical analysis. Accordingly, we believe that it is this mirror-symmetric intermediate with an acidic 16e metal center and a basic lone pair at the N atoms of the doubly-bent aryldiazenido ligand that further dimerizes to give the dibridging aryldiazenido products **2** and **3**.

Given that the dimerization produces only one type of structural isomer, the question remaining is how to explain the high stereoselectivity of this dimerization. Ideally, the dimerization of the two-legged piano stool molecule of interest (whether it be a truly chiral molecule, such as **1**, or a prochiral molecule, such as the proposed 16e intermediate) could give as many as eight different stereoisomers.²⁸ However, in practice, only two enantiomers, i.e., the RR' and SS' isomers, have been obtained. Comparing several possible pathways, we found that the one using the 16e intermediate as the starting monomer and proceeding in a nonconcerted fashion is the most chemically plausible. From this, a possible mechanism, forming **2** or **3** from **1**, is postulated and shown in Scheme 4.

In this mechanism, a pair of enantiomeric adducts are first formed by an attack from the more basic nitrogen atom (N_α) of one monomer (call it the “base”) at the acidic metal center (16e) of a second monomer (which we will call the “acid”) from either side of its two prochiral faces. It is significant that the most stable conformation of the 16e species has the aryldiazenido ligand bent away from the Cp^* . With this coordination, the metal center of the “acid” achieves a three-legged piano stool structure, i.e., becomes a chiral center. On the other hand, through the donation of the lone pair on N_α , the rotation barrier about the Ir– N_α bond in the “base” monomer, caused by an antibonding interaction between the metal d_{xy} and the lone pair orbitals as mentioned above, has been effectively removed. In other words, in order to form the second aryldiazenido bridge, the Cp^*IrX fragment of the “base” monomer could readily rotate along its Ir– N_α bond to orient its *planar* acidic metal center

Scheme 4



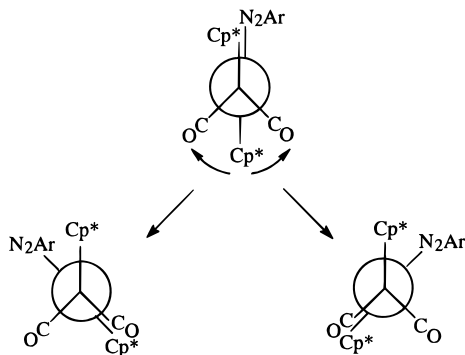
(16e) to face the doubly-bent aryldiazenido ligand of the “acid” monomer. Two opposite directions of this rotation could be possible, shown by the double-headed arrows in Scheme 4. However, one of these is more sterically hindered, first by the interaction of the rather bulky doubly-bent aryldiazenido of the “acid” moiety and the Cp^* ligand of the “base” and then by the two cis-encountered X groups. It may well be this spatial difference that practically leads to only the RR' and the SS' enantiomers as the observed products. Furthermore, since the lobe of the lone-pair orbital at the N_α atom of the “acid” monomer is pointing away whereas the lobe at the N_β atom is pointing directly toward the closing acidic metal center, the formation of a μ - η^2 -bridging aryldiazenido ligand is evident.

Formation of an analogous 16e intermediate with a doubly-bent aryldiazenido ligand could also be achieved when the metal base $Cp^*Ir(CO)_2$ (in both σ - and π -directions) was used as the ancillary ligand L . The postulated mechanism for formation of **6** from $Cp^*Ir(CO)_2$ and **1** has been shown in Scheme 1. To further illustrate the stereoselectivity of this reaction, a Newman projection along the Ir–Ir bond of the proposed 16e intermediate is shown in Scheme 5.

Once the 16e intermediate is formed, the two metal fragments linked by the Ir–Ir single bond could still rotate relative to each other. Two opposite directions of the rotation are indicated by the arrows in the scheme. When the rotation brings the aryldiazenido ligand into either of two positions trans to a CO group, a carbonyl transfer from one metal center to the other, with assistance of a synergistic coordination by the N_β of the aryldiazenido ligand, could occur, which would yield **6** as a pair of enantiomers. This synergistic process closely resembles

(27) A support for this is the series of neutral and cationic three-legged piano stool complexes $[Cp^*Ir(L_1)(L_2)(p-N_2C_6H_4OMe)]^n$ ($n = 0, +1$) given in reactions ii–v of Scheme 2. Here the ligands L_1 and L_2 have been carefully chosen to have similar σ -donating abilities and not be π -basic. The group orbitals of *in-phase* and *out-of-phase* combinations of the two σ orbitals from L_1 and L_2 closely resemble the σ -donor and π -donor orbitals of a virtual *very strong* π -base ligand that are needed to avoid a highly reactive 16e species. By comparison with the similar (unsymmetrical) orientations of the planar singly-bent aryldiazenido ligands in the X-ray structures of $[Cp^*Ir(P(p-tol)_3)(p-N_2C_6H_4OMe)]^+$ and **1**,^{4a,5} the plane containing the doubly-bent aryldiazenido ligand in the molecular structure of $[Cp^*Ir(PMe_3)_2(p-N_2C_6H_4OMe)]^+$ is indeed rotated through 90° so as to be symmetrical, i.e., lying in the plane through Ir and bisecting the two PMe_3 groups.⁵

(28) When the two aryl groups are trans to each other, four different stereoisomers (assigned as RR' , RS' , SR' , and SS') based on the chirality of the iridium atoms in the dimers can be deduced. Similarly, another four different stereoisomers can be obtained by a *cis* arrangement of the two aryl groups.

Scheme 5. Stereoselectivity of CO Transfer

the terminal–bridging–terminal carbonyl exchange process described by Cotton.²⁹

Conclusion

In this work, the strong π -base ligands I^- , Br^- , and $Cp^*Ir(CO)_2$ have been separately used to replace the ethylene ligand in $[(\eta^5-C_5Me_5)Ir(C_2H_4)(p-N_2C_6H_4OMe)][BF_4]$ (**1**), yielding the diiridium complexes $[(\eta^5-C_5Me_5)IrX]_2(\mu-\eta^2-p-N_2C_6H_4OMe)(\mu-\eta^1-p-N_2C_6H_4OMe)$, $X = I$ (**2**) and Br (**3**), and $[(\eta^5-C_5Me_5)Ir(CO)]_2(\mu-\eta^2-p-N_2C_6H_4OMe)[BF_4]$ (**6**). The π effect of the ancillary ligand on the geometric transfer of the aryldiazenido ligand, observed in these reactions, has been rationalized in terms of molecular orbital interactions in a molecule of the general formula $(\eta^5-C_5Me_5)Ir(L)(p-N_2C_6H_4OMe)$. It is concluded that when L is a strong π -base, the aryldiazenido ligand prefers a doubly-bent geometry and this may be accomplished

by a thermal electron transfer process. By a comparison with previous results in this series,^{4,5} where a weak π -acid was used as L and a singly-bent geometry for the aryldiazenido ligand was retained, the geometric and electronic influences of the ancillary ligand on the metal–diazenido bonding have been systematically discussed. Spectroscopic data have shown that **2** and **3** are isostructural. Single-crystal X-ray crystallographic analyses of **2** and **6** have been accomplished and documented. ¹H and ¹⁵N NMR studies of the protonation reactions of **2** and **3** indicate that the protonation occurs at the N_α nucleus of the $\mu-\eta^2-p-N_2C_6H_4OMe$ ligand and not at that of the $\mu-\eta^1-p-N_2C_6H_4OMe$ group.

Finally, to the best of our knowledge, complexes **2** and **3** reported in this work are the first two examples of compounds having two coordinatively different bridging aryldiazenido ligands. Also, complex **6** is only the second example having a $\mu-\eta^2$ -bridging aryldiazenido ligand.^{7a}

Acknowledgment. We thank the Natural Sciences and Engineering Research Council of Canada for support of this work through research, equipment, and infrastructure grants to F.W.B.E. and D.S. and Johnson Matthey & Co. for a generous loan of iridium trichloride.

Supporting Information Available: For compound **2**, text giving the detailed crystallographic analysis and listings of fractional atomic coordinates and isotropic or equivalent temperature factors for the non-hydrogen atoms (Table S1), fractional atomic coordinates and isotropic temperature factors for hydrogen atoms (Table S2), and anisotropic thermal parameters (Table S3) and, for compound **6**, text giving the detailed crystallographic analysis and a listing of fractional atomic coordinates and isotropic or equivalent temperature factors for the non-hydrogen atoms (Table S4) (11 pages). Ordering information is given on any current masthead page.

(29) Cotton, F. A.; Wilkinson, G. *Advanced Inorganic Chemistry*, 5th ed.; John Wiley & Sons: New York, 1988; p 1327.